Behavioral/Cognitive

Motion Makes Sense: An Adaptive Motor-Sensory Strategy Underlies the Perception of Object Location in Rats

Inbar Saraf-Sinik,* Eldad Assa,* and Ehud Ahissar
Department of Neurobiology, Weizmann Institute of Science, Rehovot 76100, Israel

Tactile perception is obtained by coordinated motor-sensory processes. We studied the processes underlying the perception of object location in freely moving rats. We trained rats to identify the relative location of two vertical poles placed in front of them and measured at high resolution the motor and sensory variables (19 and 2 variables, respectively) associated with this whiskers-based perceptual process. We found that the rats developed stereotypic head and whisker movements to solve this task, in a manner that can be described by several distinct behavioral phases. During two of these phases, the rats' whiskers coded object position by first temporal and then angular coding schemes. We then introduced wind (in two opposite directions) and remeasured their perceptual performance and motor-sensory variables. Our rats continued to perceive object location in a consistent manner under wind perturbations while maintaining all behavioral phases and relatively constant sensory coding. Constant sensory coding was achieved by keeping one group of motor variables (the "controlled variables") constant, despite the perturbing wind, at the cost of strongly modulating another group of motor variables (the "modulated variables"). The controlled variables included coding-relevant variables, such as head azimuth and whisker velocity. These results indicate that consistent perception of location in the rat is obtained actively, via a selective control of perception-relevant motor variables.

Key words: **active touch; motor-sensory control; sensory coding; whisking; perceptual constancy; proximal stimulus**

Introduction

Perception is a process by which the brain obtains information about the environment. In natural conditions, perception typically entails an iterative interplay between sensor motion, the environment, and the resulting sensory activation. The motor component of this interplay possesses the potential for selecting the information that is most relevant to the task at hand, and provides the flexibility necessary to reliably acquire it, and for maintaining consistent perception despite changes in the environment. Here we address the control of perception-targeted movements in freely moving rats performing an object localization task under different environmental conditions.

The rodent's whisking system has become a widely used model for studying mechanisms of perception in the last two decades (Diamond et al., 2008; Prescott et al., 2011; Maravall and Diamond, 2014). Numerous studies have demonstrated the usage of rats' facial vibrissae in various perceptual tasks, such as object localization (Knutsen et al., 2006; Mehta et al., 2007; Ahissar and Knutsen, 2008; Knutsen and Ahissar, 2009; O'Connor et al., 2010), shape discrimination (Brecht et al., 1997; Anjum et al., 2006), and texture discrimination (Carvell and Simons, 1990; von Heimendahl et al., 2007; Ritt et al., 2008; Wolfe et al., 2008; Diamond, 2010; Maravall and Diamond, 2014). Several studies characterized whisking behavior in freely behaving animals (Mitchinson et al., 2007; Towal and Hartmann, 2008; Grant et al., 2012), and others characterized motion-induced mechanical interactions between whiskers and objects (Boubenec et al., 2012; Quist and Hartmann, 2012; Bagdasarian et al., 2013; Hires et al., 2013; Pammer et al., 2013). Yet, the association between a well-defined motor routine and the perception of specific features of external objects was only rarely addressed (one recent example is the study by Voigts et al., 2015).

Similar to motor tasks, perceptual tasks are under active control of the CNS and their accuracy depends on the functioning of both motor and sensory components. Studies of motor tasks (Shadmehr et al., 2010), perceptual tasks (Saig et al., 2012), and optimal control theory (Todorov, 2004) suggest two major types of motor variables that can be measured during the performance of a given task: "controlled variables," which the system aims to maintain within a given range or a trajectory; and "modulated variables," which the system adjusts to keep the controlled variables within these desired ranges. The current study examined the control of motor variables and its effect on sensory coding in tactile-based spatial perception.

We obtained whisking-related motor and sensory variables from rats performing an object localization task in normal conditions and while facing external wind perturbations. We found

Received Oct. 7, 2014; revised April 19, 2015; accepted April 21, 2015.

Author contributions: I.S.-S., E. Assa, and E. Ahissar designed research; I.S.-S. and E. Assa performed research; I.S.-S. and E. Assa analyzed data; I.S.-S., E. Assa, and E. Ahissar wrote the paper.

This work was supported by Israel Science Foundation Grant 1127/14, the Minerva Foundation funded by the Federal German Ministry for Education and Research, the United States-Israel Binational Science Foundation Grant 201143, the National Science Foundation-Binational Science Foundation Brain Research EAGER Program Grant 2014906, and the Office of the Chief Scientist the Israeli Ministry of Health. E. Ahissar holds the Helen Diller Family Professorial Chair of Neurobiology.

The authors declare no competing financial interests.

*I.S.-S. and E. Assa contributed equally to this study.

Correspondence should be addressed to Dr. Ehud Ahissar, Department of Neurobiology, Weizmann Institute of Science, Rehovot 76100, Israel. E-mail: ehud.ahissar@weizmann.ac.il.

DOI:10.1523/JNEUROSCI.4149-14.2015

 0270-6474/15/358777-13$15.00/0

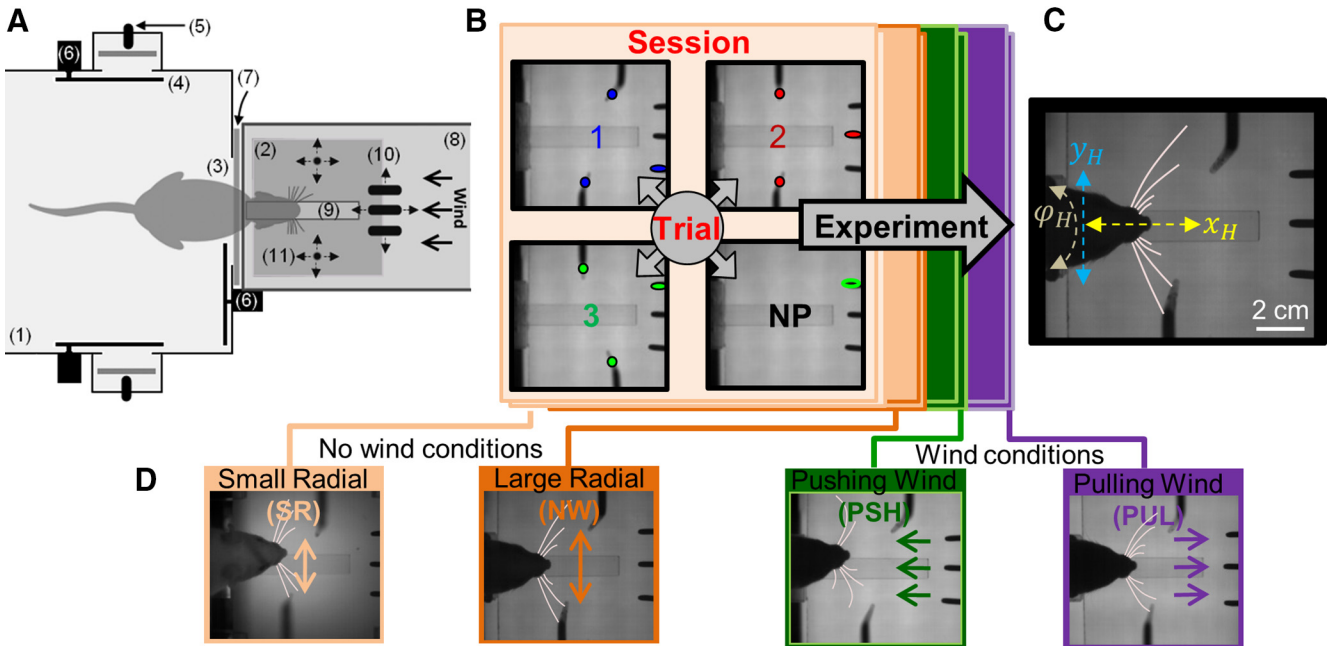

Figure 1. Task set, arrangements, and conditions. ***A***, Behavioral setup, including (1) arena, (2) task area, (3) front door, (4) side opening, (5) side sipper, (6) motorized door, (7) IR beam sensor, (8) wind tunnel, (9) bridge, (10) 3 front drinking tubes (sippers), and (11) poles (arrows indicate possible motion directions). ***B***, Task area in the four possible trial arrangements: poles arrangement 1 (blue), 2 (red), and 3 (green), and no poles (NP, black). Colored symbols represent the location (top view) of the two poles at the height of whisker contacts and the sipper associated with each arrangement. Sessions (including trial repetitions of all 4 arrangements) are 1 of 4 conditions (block design; see ***D*** for blocks' color code). ***C***, One frame, showing the task area during arrangement 1 trial. Dashed arrows indicate head motion axes: along task progress (x_H), along the mediolateral axis (y_H) and azimuthal angle (φ_H). ***D***, Snapshots from sessions under different conditions: two no wind conditions, different in radial distance of the poles: small radial (SR) and large radial in no wind (NW). Two wind conditions, pushing (PSH) and pulling (PUL), different in wind direction (marked by colored arrows).

that our rats used a motor-sensory control scheme that maintains perception-relevant motor variables within task-relevant ranges while modulating other motor variables. As a result, the peripheral sensory coding of the relevant environmental variables remained resilient to external perturbations.

Materials and Methods

Rats. Four female rats (8 weeks old) were trained in the object detection and localization tasks. Rats were held 2 in a cage, under a 12 h light-dark cycle. They were given free access to food and were gradually engaged in a water scheduling protocol, eventually allowed access to fluids during and depending on task performance (conditioned) and, additionally, in the home cage for 2 h per day (unconditioned). After learning the task (see below), rats were trimmed of all whiskers, except row C, and retrained until performance stabilized again. Trimming was repeated throughout data collection period as needed to maintain the rats with only C row intact with no additional training.

Experimental apparatus. The experimental apparatus (Fig. 1*A*) was set inside an acoustically isolated, lightproof chamber and included two distinct areas: "arena" and the "task area," connected by a door ("front door"). Upon door opening, rats entered the task area to perform a trial and, if successful, were rewarded with mango-flavored juice (reward) via one of three front metal drinking tubes ("sippers"). Each sipper was electrically connected to an adjustable capacitance switch (F53N; David Johnson & Associates), used as a contact detector to condition juice delivery. Solenoid valves (360P012-42; NResearch) controlled reward delivery (volume, timing). Next, rats were called back into the arena via signaling of a second reward ("side") and upon their return the front door closed. Motorized doors (HS-300; Hitec) controlled the passage between spaces and IR beam sensors (E24-01 Optical Lickometer; Coulbourn Instruments) reported crossing through. Rats performed 30–120 (typically ~60) trials in one session (25–60 min), consuming 5–15 ml juice. Sessions were terminated, when rats stopped performing the task for 3 consecutive trials. The task area was enclosed by a square transparent wind tunnel (15 × 15 × 70 cm), in which a computer-controlled fan (172 × 150; 60VDC fan; Y.S. Tech) provided air flow in wind sessions in one of two directions: against ("pushing wind") or with ("pulling wind") the motion of rats as they entered the task area.

High-speed camera (MotionPro; Redlake) located above the task area recorded video movies of rats performing the task at high spatiotemporal resolution (500 fps, 740 × 896 pixels). Another infrared-sensitive CCD camera (55–701; Edmund Industrial Optics) allowed monitoring of behavior in the arena. IR backlight led array (830 nm, MB-OBL9x9-IRN-24-1 V OmniLight flat dome; Metaphase Technologies) illuminated the task area, and a 10 × 10 cm array of infrared (940 nm) LEDs (L940-04AU; Epitex) illuminated the arena. None provided visible illumination for the rats, which performed the task in complete darkness, but provided illumination visible by the cameras' sensors. A narrow plastic bridge (1.5 × 12 cm) allowed passage from the front door to the far end of the task area. Along the bridge, two vertical metal poles (2.8 mm diameter) were presented: one on each side, at different spatial arrangements. Each of the two poles, as well as the front sippers were mounted on *x-y*-axes computer-controlled mobile tables (FB075-150-1.0M4 Nanomotion Linear Stage; Abiry Technologies), which allowed *x-y* positioning of 1 μm precision.

Training. First, rats learned to alternate between the arena and task area, allowing a structured partition of the session to discreet trials of recurring task performance.

The second stage of training, the discriminative training, included two trial types: "poles trials," in which two vertical poles were bilaterally positioned in the rats' path; and "no poles trials," in which rats were let to explore a clear path. In the poles trial, the poles were positioned in one of several possible arrangements, each associated with a different one of three available front sippers ("correct sipper"; Fig. 1*B*).

Association was gradually achieved by first offering reward from the correct sipper. Gradually, as rats learned the associations, they chose a sipper before reward administration, and reward administration was conditioned on rats' choices.

Task. Before each trial, one poles-sipper arrangement was chosen from a set of arrangements between which rats had learned to discriminate.

Arrangements were presented in a semirandom order along a session (Fig. 1*B*), controlling equal probability of each sipper to be correct and one-sixth probability of no poles arrangement to be presented. Once selected, the poles and front sippers were simultaneously moved to a reference point, common to all arrangements in the set, and then to their final positions to prevent any auditory cues that may be informative. Then, the front door opened and rats had to explore the task area and choose the sipper corresponding to the presented arrangement. Then rats reentered the arena to collect the side reward. Failing to choose the correct sipper led to withdrawal of both front and side rewards and to an increased time delay of the following trial.

Time limits were assigned for each of these stages (5–10 s for each stage). Failing to complete one of these stages before reaching its time limit led to trial termination. Data of rats performing the task were collected under the following four conditions (Fig. 1 *B*, *D*):

1. Arrangements with small radial distance (each, 20–23 mm from midline, laterally, small-radial condition).
2. Arrangements with large radial distance between the poles (each, 25–29 mm from midline, laterally) and no wind applied (no wind condition).
3. Arrangements with large radial distance and with wind applied against the direction of movement toward the front sippers (pushing wind condition).
4. Arrangements with large radial distance and with wind applied with the direction of the movement toward the front sippers (pulling wind condition).

Poles arrangements were of the same radial distance (e.g., 29 mm from midline laterally), but a different horizontal distance (along the rostrocaudal axis). The most posterior pole, however, was always positioned at a fixed distance from the front door (5.5 cm). The horizontal offset between the poles was 0 or ±20 mm.

Wind in both directions was applied by a fan, located at the end of the wind tunnel. Wind velocities were mapped by an anemometer, positioned at the center-most posterior point of the task area, at a typical height of a rat's head as it goes out. At this point, typical wind velocities were measured 3.5 m/s at the pushing wind condition and 2.5 m/s at the pulling wind condition. Wind was applied continuously throughout dedicated sessions to mimic a consistent change in environmental conditions.

Study groups. The experiment included two study groups: the three alternative forced-choice (3-AFC) version, trained to discriminate between a set of three poles arrangements (1–3; Fig. 1*B*), where the correct sipper headed isosceles triangles created between the two poles and the correct sipper, and a no poles arrangement that was associated with sipper 1 or 3 for different rats. Rats in the two alternative forced-choice (2-AFC) version discriminated between arrangements 1 and 3. In no poles trials, they were free to choose any of the available sippers.

Controls. Two types of controls were designed to verify the following: (1) rats based their decision on the locations of the poles; and (2) sensory information was acquired by using their whiskers. In one, poles were removed from the *x*-*y* motors, maintaining all other cues (e.g., auditory, smell) intact; and in the second, rats were trimmed of all their whiskers. Controls were limited to single sessions each, to avoid frustration of the rats, and to prevent them from evolving a new behavioral strategy, such as using their paws or snouts instead of their whiskers, to solve the task.

Data acquisition. Behavioral events (crossing through a door, licking on a sipper) were tracked via IR beam sensors and capacitance switches. Their respective time stamps were logged as was trial relevant information (e.g., arrangement's ID, chosen sipper, etc.), for performance analysis. Video files of rats performing the task were acquired by the high-speed camera and automatically saved upon trigger using the MIDAS software.

Data analysis: success rates quantification. Performance level was evaluated as the ratio between correct sipper selections and the number of trials in a session. Chance level performance was calculated for individual sessions, as the sum of probabilities for arrangement i to appear in a session ($P_{a_i} = a_i/\sum_j a_j$, where a_i is the number of arrangement i trials in the session) and the sipper i to be selected ($P_{s_i} = s_i/\sum_j s_j$, where s_i is the number of sipper i selections in a session), assuming no interaction between the two; thus, chance level is $\sum_i P_{a_i} P_{s_i}$. p values for interaction between arrangements and sipper choices distribution were calculated using χ^2 test for pairs of sequential sessions to get sufficiently large number of trials to satisfy a valid statistical test. All other statistical comparisons were based on ANOVA, unless mentioned otherwise.

Table 1. Definition of variables

Notation	Definition
Head variables	
x_H	Head position along the *x*-axis
y_H	Head position along the *y*-axis
$\dot{x}_H$	Head velocity along the *x*-axis
$\dot{y}_H$	Head velocity along the *y*-axis
φ_H	Head azimuth
φ_{H,C_S}	Head azimuth at short contact onset
φ_{H,C_L}	Head azimuth at long contacts onset
Whisker variables	
$T_{W,prt}$	Whisker's duration of protraction
$T_{W,ret}$	Whisker's duration of retraction
$A_{W,prt}$	Whisker's amplitude during protraction
$A_{W,ret}$	Whisker's amplitude during retraction
θ_W	Whisker angle (relative to head midline)
$\theta_{W,max}$	Whisker angle at peak protraction
$\theta_{W,min}$	Whisker angle at peak retraction
$\dot{\theta}_W$	Whisker angular velocity
$\dot{\theta}_{W,max}$	Whisker's maximal velocity during protraction
$\dot{\theta}_{W,min}$	Whisker maximal velocity during retraction
$\bar{\dot{\theta}}_{W,prt}$	Whisker's averaged velocity during protraction
$\bar{\dot{\theta}}_{W,ret}$	Whisker's averaged velocity during retraction
Contact variables	
r_{C_S}	Radial distance of short contacts
r_{C_L}	Radial distance of long contacts
T_{C_S}	Contact duration of short contacts
r_{C_L}	Contact duration of long contacts
Sensory coding variables	
$\Delta\theta_{onset}$	Angular difference between the contacting whisker and its homolog (not necessarily contacting) whisker on the other side, at the time of contact onset
Δt_{onset}	Time delay between two sequential contralateral contacts

Tracking. Head and whisker motion during task performance was tracked offline using MATLAB-based software (WhiskerTracker) (Knutsen et al., 2005), a semiautomatic head and whiskers tracker. For measurement and definitions of head position, head azimuth, and whisker angle, see Knutsen et al. (2005).

Head motion variables. Head trajectories were extracted from the movies in video based coordinates (pixel units) and transformed to "real-world" coordinates (distance from entrance point to task area, cm units). Pixel to cm transformation was calibrated with respect to the plastic bridge, which was a constant object in the field. The task area was thereafter described in 2D coordinate system along two axes: *x* and *y* (Fig. 1*C*).

Before analysis, head traces were low pass filtered at 50 Hz (MATLAB *filtfilt* function). Four head motion variables were measured and further analyzed: head trajectory (head positions of the *x* (x_H) and *y* (y_H) axes, head azimuthal angle (φ_H), head velocity (the time derivative of head position along the *x*-axis [$\dot{x}_H$] and *y*-axis [$\dot{y}_H$]) (Table 1).

These traces were then resampled with respect to *x*-axis (MATLAB *spline* function); the longest section from each trial, where x_H monotonically increased, was chosen and further processed. This resulted in removal of ~6% and ~20% (in average) of tracked data from the beginning the end, respectively. The latter section included mostly the stage of reward collection. Averages of head motion variables were considered valid only when the number of samples (n) was ≥30.

Trials where head position or head azimuth deviated from the average (calculated separately for each poles-sipper arrangement) in >3 SDs, in one point or more along the *x*-axis, were excluded from further analysis (~6% of the trials).

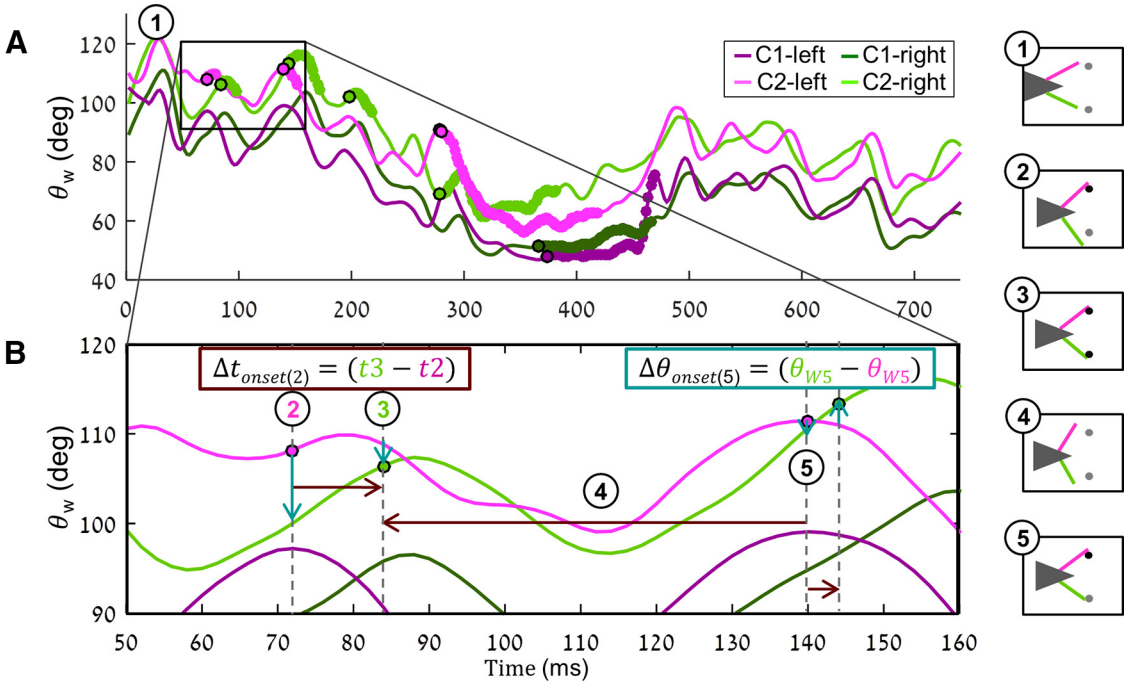

Figure 2. Measurement of sensory coding variables: Δt_{onset} and $\Delta\theta_{onset}$. ***A***, Four whisking traces showing whisker angles (θ_W vs time) of left (purple) C1 (dark) and C2 (light), and right (green) C1 (dark) and C2 (light) whiskers, during task performance. Thick segments represent a contact of the relevant whisker with the pole. Black symbols represent the onset of contacts. ***B***, Magnification of the area in ***A***, marked with black rectangle. Filled symbols represent the onsets of contacts. Arrows indicate Δt_{onset} (red) and $\Delta\theta_{onset}$ (cyan). Arrows' lengths correspond to the time elapsed between a contact and the following contralateral contact (Δt_{onset}), or the angle difference between two homolog whiskers ($\Delta\theta_{onset}$). Arrows' direction indicates the sign according to convention, by which left side values are subtracted from right sides values; thus, the left pointing arrows mark a right side lead (negative Δt_{onset}) and down pointing arrows, a more protracted left side (negative $\Delta\theta_{onset}$). Measurements of Δt_{onset} and $\Delta\theta_{onset}$ are demonstrated for points 2 and 5, respectively (thick arrows, formulas). The numbered illustrations on the right demonstrate the position of rat's head (triangle) and whiskers (light purple and green lines) and the two poles during contacts (circles, black) or no contacts (gray), during the time points with the corresponding numbering on ***A*** and ***B***.

Whisking motion variables. Whisker angle traces were smoothed using quadratic fit with a moving window, 5% width (MATLAB *malowess* function), and further analyzed. Individual traces were each partitioned into three segment types, based on the sign and magnitude of whisker angle velocity ($\dot{\theta}_W$). Segments were defined as "protraction" ($\dot{\theta}_W >$ th), "retraction" ($\dot{\theta}_W <$ -th), or "break" otherwise, with th = 100°/s. Segments, lasting <6 ms (3 frames), were reassigned as part of the proximal former segment. For each protraction and retraction segment, the following variables were measured: peak (protraction) and trough (retraction) angle, amplitude, duration, and averaged and maximal velocities (Table 1).

Contact variables. Manual video-based analysis produced onset and offset frames of whisker-pole contact events and assigned each to the contacting whisker. For each contact event, we measured the duration and radial distance of contact, as well as related whisking and head variables at the time of contact (Table 1).

Definitions and calculations of sensory coding variables (Δt_{onset} and $\Delta\theta_{onset}$). Information regarding the horizontal offset between the poles (Δx) can be actively represented by the whisking system in the spatial domain and/or in the temporal domain (Fig. 2). In the spatial domain, Δx is represented by the angle difference between homolog whiskers at the time of contact, $\Delta\theta_{onset}$ (Fig. 2*B*, point 5, where the two C2 whiskers are with the same angle, corresponding to poles' offset of 0 degrees). The temporal cue that is available to the system is the time delay between two sequential contralateral contacts, Δt_{onset} (Fig. 2*B*). When the whiskers in both sides of the pad move synchronously Δt_{onset} directly represents Δx. By convention, values on the left side are subtracted from those on the right side; thus, negative Δt_{onset} or $\Delta\theta_{onset}$ values (Fig. 2, left pointing and downwards pointing arrows, respectively) denote cases in which contact on the right preceded that on the left, or cases where whisker angle was larger on the left side, respectively. Contact events, which were not followed by a contralateral contact, were regarded unilateral and omitted from statistical analysis.

Definition of phase transition points between behavioral phases. Transition points between behavioral phases along task progress were defined as follows: For Phases 1 and 2 and Phases 3 and 4, the transition was defined at 0.9 of the mode of the first contact position and last head turn respectively; for Phases 2 and 3, the phase transition was defined at 0.9 of the peak of the long contacts histogram along the *x*-axis.

Results

Highly trained rats discriminated between several spatial arrangements of two vertical poles by choosing one of three available drinking tubes ("sipper"), based on prelearned associations (Fig. 1*A*,*B*). Two rats (CV12, CV13) performed a 3-AFC task, discriminating between 3 poles arrangements (arrangements 1, 2, 3) and a fourth, no poles arrangement. These rats yielded 8572 trial repetitions and 1413 s of tracked video data. Two rats (CV15, CV18) performed the 2-AFC task (discriminating between arrangements 1, 3) and yielded 10541 trial repetitions and 385.2 s of tracked video data.

Throughout data collection, performance was above chance level for all rats and in all conditions, as illustrated for CV13 (Fig. 3*A*; $p < 10^{-6}$, χ^2 test). No poles trials, in which detection rather than localization was required, were introduced in one-sixth of the trials (see Materials and Methods). Success rates in no poles trials were significantly higher than in poles trials (0.92 ± 0.11 vs 0.66 ± 0.13; mean ± SD session success rate; $p < 10^{-10}$, ANOVA), indicating that detection was easier than localization for our rats. Further, assuming equivalent training, 2-AFC was easier than 3-AFC (Fig. 3*B*; 0.86 ± 0.1 compared with 0.71 ± 0.09; $p < 10^{-6}$). Control experiments, in which all whiskers were trimmed or in which poles were removed, demonstrated that

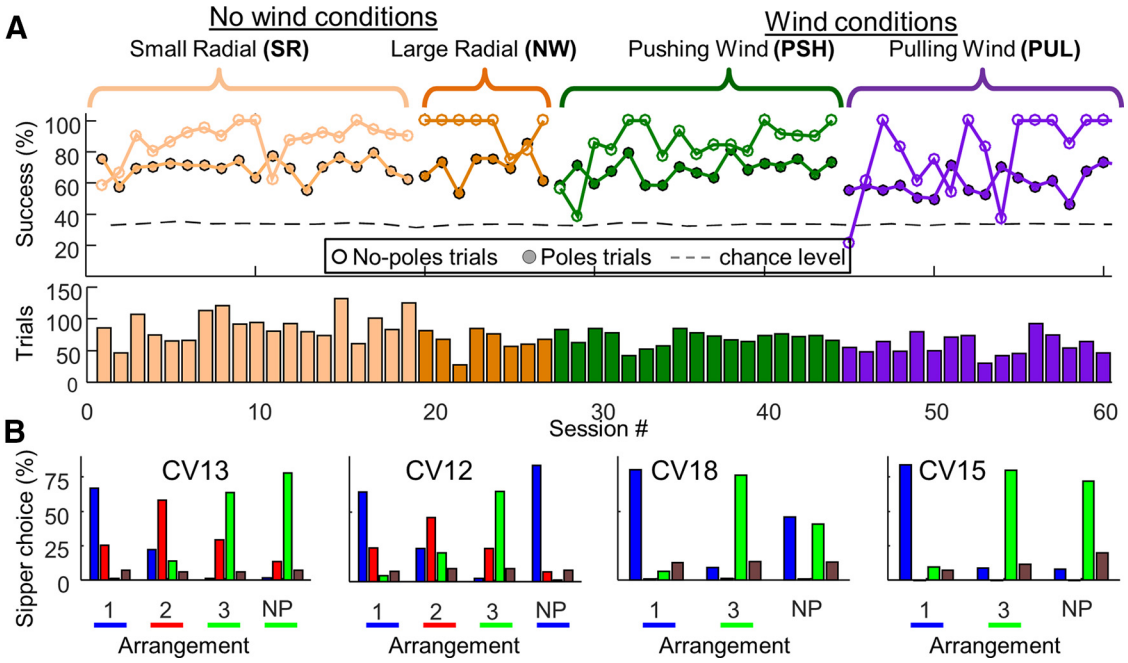

Figure 3. Task performance. ***A***, Success rates (CV13, top): poles trials (closed symbols) and no poles trials (opened symbols). Dashed gray line indicates chance level. Number of trials/session (bottom) in the four conditions along the experiment. ***B***, Rats' choices of sippers 1–3 (blue, red, and green, respectively) or no choice within the allocated time (brown), pulled over all conditions for rats (left to right) CV13, CV12, CV18, and CV15. Colored horizontal bars represent the correct choice for each arrangement and for each rat. Bar absence indicates that no specific sipper was associated. NP, No poles.

these rats relied on whisker-pole interactions for solving the task (data not shown).

General behavioral strategy

To analyze the strategy used by our rats while perceiving object locations, we measured trajectories of head and whisker motion variables along the main axis of task progress (x), during trials of the four arrangements (arrangements 1, 2, 3, and no poles). Single trials exhibited arrangement-specific trajectories in head position (x_H, y_H; Fig. 4*A*, Rat CV13), head velocity along the y-axis ($\dot{y}_H$), and head azimuth (φ_H). Examination of the mean position profiles (over trials of each arrangement) revealed a stereotypic head motion along a common trajectory, from which it deviated, in an arrangement-specific manner, at two points (Fig. 4*B*); in no poles trials, the head deviated toward the associated sipper earlier (smaller x_H) than in poles trials, suggesting that a detection phase preceded localization in this paradigm. This was evident also in $\dot{y}_H$ (Fig. 4*C*) and φ_H (Fig. 4*D*) mean profiles. Analysis of whisker contacts showed that rats first contacted the poles before the point of first deviation (Fig. 4*E*) and continued to make contacts with the poles along the range extending between the two deviation points (Fig. 4*F*), outlining this range as related to localization. Along this localization range, rats exhibited two types of contacts: early, short contacts (duration <50 ms), and late, long contacts (typically 50–200 ms; Fig. 4*F*). Whisker peak angle ($\theta_{W,max}$) also exhibited a stereotypic pattern: the rat started with large (protracted) angles and gradually reduced them (Figs. 4*G*, 5*A*), regardless of the actual occurrence of whisker-pole contact, as evident from the consistent trend in no poles trials.

This stereotypic behavior can be parsed into five sequential phases (Fig. 4*A–I*, gray shadings), as follows: The first phase, detection, was characterized by protracted set-points of the whiskers and large whisking amplitudes, which then decreased in expectation of contact with the poles (Fig. 4*G*; single-trial examples are shown in Figs. 4*I*, 5*A*,*B*). Bilateral symmetry of whisking during detection largely varied between trials, being in phase or completely antiphased (Fig. 5*A*). The beginning of the second phase, localization, was defined as the position of the head at first contact. The typical position along the x-axis where phase transition occurred was determined for each rat based on the distribution of x_H at the point of first contact (Fig. 4*H*).

Poles' location was acquired by the rats along two sequential phases: during the early phase (Phase 2), head was aligned between the poles (Fig. 4*B*), orienting forward (Fig. 6*A*), and whisking angles were identical between arrangements (Fig. 6*B*). During late localization phase (Phase 3), head trajectories diverged in an arrangement-specific manner (Fig. 6*A*), whiskers developed an arrangement-specific bilateral asymmetry (Fig. 6*B*), and the probability of long whisker-pole contacts increased (Fig. 4*F*). The transition between Phase 2 and Phase 3 was determined as the point along the x-axis in which the number of long contacts reached 0.9 of its maximal value (Fig. 4*F*,*H*).

The rats controlled their locomotion speed while performing the task. Importantly, forward locomotion ($\dot{x}_H$) was slowed down during Phase 2, such that more time was devoted to early localization than to late localization (Fig. 5*B*). The transition from Phase 2 to Phase 3 was also characterized by small arrangement-specific deviations of head variables (Fig. 4*B–D*), which were later amplified at the end of Phase 3.

The fourth phase, choice execution, was characterized by a ballistic-like profile of head velocity $\dot{y}_H$ (Fig. 4*C*), toward one of the sippers. The transition point between Phases 3 and 4 was defined as the point along the x-axis of last direction change. Last, Phase 5 was reward collection, where reward administration depended on active licking of the correct sipper, often including a brief position correction (Fig. 4*B*,*D*).

These five behavioral phases could be identified in the two 3-AFC rats in all three conditions (Table 2); representative snapshot of Rat CV13 is depicted in Figure 4*I*.

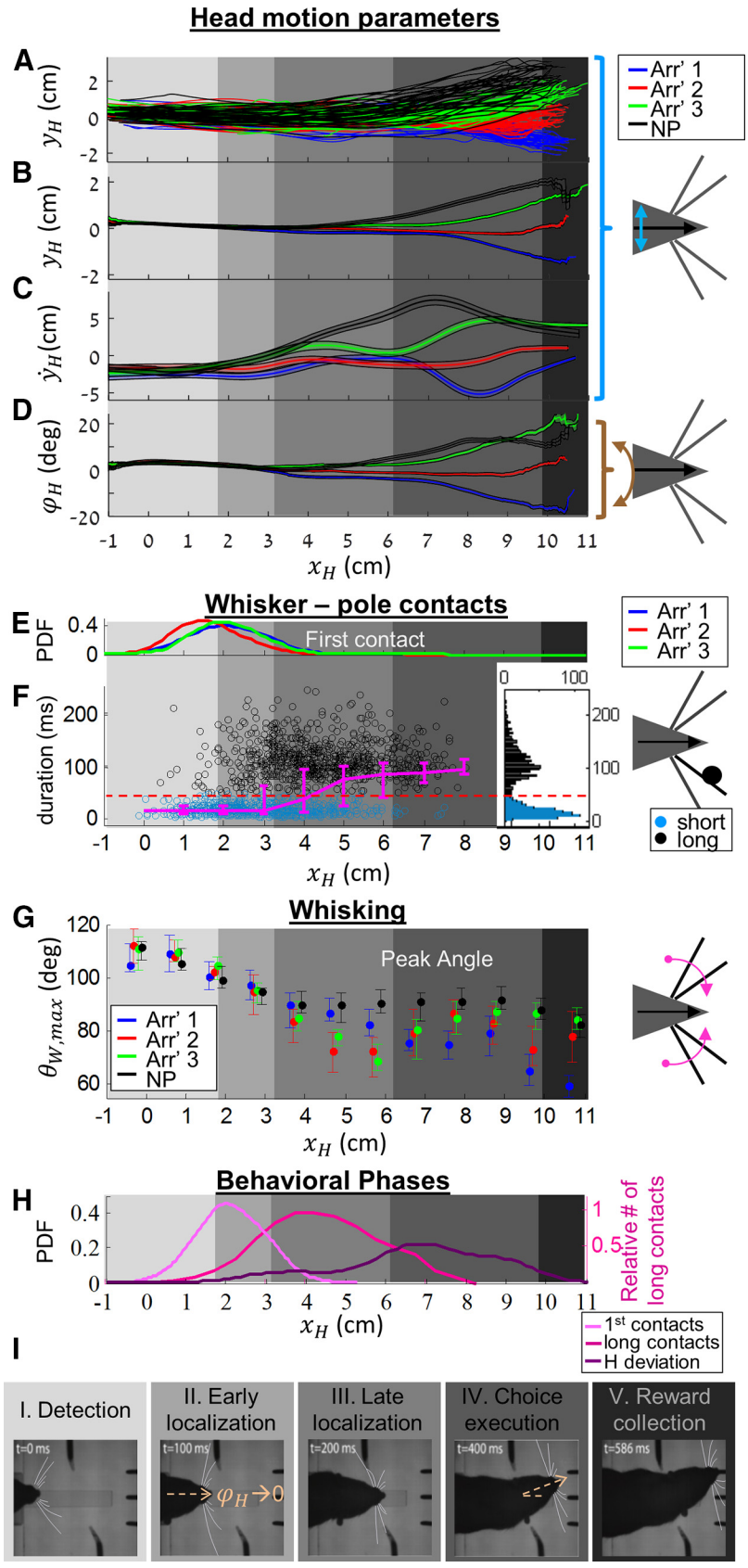

Figure 4. Five behavioral phases along task progress. ***A***, Head position trajectories in poles arrangements 1 (blue), 2 (red), 3 (green), and in no poles arrangements (black). ***B***, Position trajectories (mean ± SEM), averaged across trials of the same arrangement. ***C***, Same as in ***B*** for head velocity along the *y*-axis ($\dot{y}_H$, axis' direction is illustrated by cyan arrow on the right). ***D***, Head azimuth (φ_H, brown arrow on the right illustration) with consistent color coding. ***E***, Probability distribution function (PDF) of first contacts location along task progress, in trials of arrangements 1–3 (blue, red, and green). ***F***, Short (cyan) and long (black) contact duration values, median ± IQR (magenta) along task progress. Dashed red line indicates 50 ms cutoff between the short and long populations. Inset, Bimodal contact duration distribution (*y*-axes of the two graphs are contact duration). ***G***, Median and IQR of left C1 peak whisker angle values in arrangements 1 (blue), 2 (red), 3 (green), and no poles (black). ***H***, Transition points between behavioral phases. Phases 1 and 2: PDF of head position at first contact (light pink). Phases 2 and 3: normalized number of long contacts along the *x*-axis (dark pink). Phases 3 and 4: PDF of head position at last head turning point along the *x*-axis (purple). ***I***, Sequential snap shots from an arrangement 3 trial performance, illustrating head and whisker characteristic motion along different behavioral phases of task progress. In all panels, different gray level shadings represent the different phases (as defined in ***H***).

Localization strategy

We further examined the differences in motor-sensory strategies underlying the two localization phases and the resulting task relevant information. During early localization (Phase 2), several variables exhibited a common pattern across all arrangements. Primarily, the head was aligned between the poles ($\varphi_H \rightarrow 0$) and the whiskers were symmetrically aligned during precontact whisking ($\Delta\theta \rightarrow const$) and during contact onset ($\Delta\theta_{onset} \rightarrow const$) (Fig. 6*A–C*). Conversely, in the late localization phase (Phase 3), all spatial variables deviated in an arrangement-specific manner, with the deviation of $\Delta\theta$ eventually representing poles' offsets, Δx.

The preservation of head azimuth and $\Delta\theta$ during Phase 2 enabled a reliable representation of Δx by Δt_{onset}, which was degraded in Phase 3 (Fig. 6*D*). Short contacts were used from the first contact and throughout both localization phases; short contacts probably depended on active whisking as they could not have been reproduced when assuming the same parameters of head motion and passive whiskers, whereas long duration contacts started almost exclusively in Phase 3 (Fig. 4*F*) and did not require active whisking (data not shown). In addition, long contacts were of significantly smaller whisker angles (θ_W) and shorter radial distances (C_r, the point along the whisker of contact with the pole; data not shown).

We analyzed the dynamics of temporal and spatial cues and measured the amount of information they carried. The absolute value of Δt_{onset} gradually decreased, whereas that of $\Delta\theta_{onset}$ gradually increased with respect to x_H (Fig. 6*E*, top; binned at 0.5 cm). Mirroring trends were exhibited by the mutual information between these sensory variables and arrangement (Fig. 6*E*, middle) or sipper choice (Fig. 6*E*, bottom), with informa-

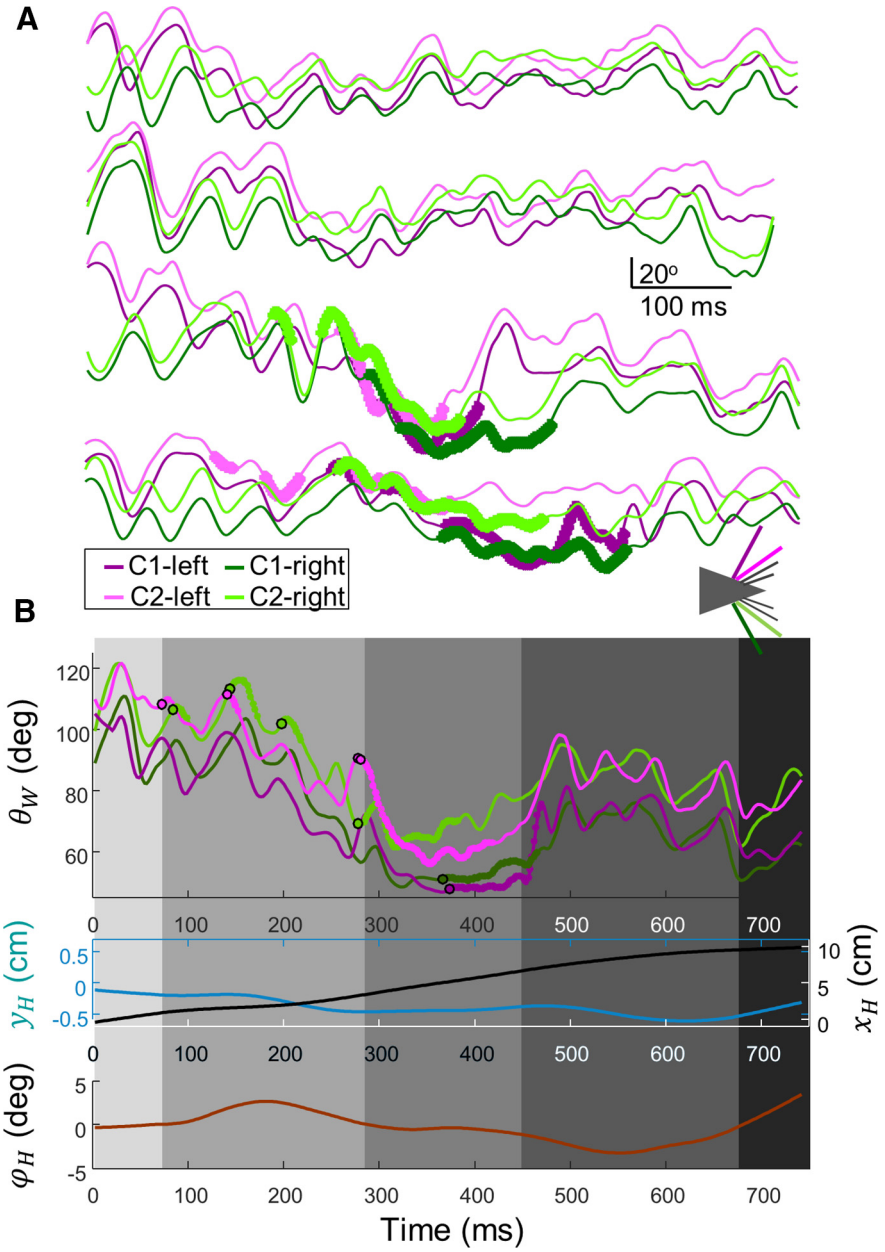

Figure 5. Typical whisking and head motion along task progress. ***A***, Examples of whisking traces (θ_W vs time) of C1 (dark) and C2 (light) whiskers of the left (purple) and right (green) sides from no poles arrangements (top two) and poles arrangements (bottom two). Thick sections represent the periods of whisker-pole contacts. ***B***, Whisking traces (consistent color code) as recorded in an arrangement 2 trial. Simultaneous head motion shown below. Cyan represents y_H. Black represents x_H. Brown represents φ_H.

tion by Δt_{onset} gradually decreasing and by $\Delta\theta_{onset}$ gradually increasing. The dynamics of the encoding power of these sensory variables along task progress is illustrated by the arrangement-wise separation of their distributions (Fig. 6*F*). The mutual information between head azimuth (φ_H) and arrangement or sipper choice gradually increased with task progress, starting upon the diminishing of the information contained in the temporal variable and continuing until the end of the trial (Fig. 6*E*).

Wind perturbation

Wind perturbation did not qualitatively change the general structure of the behavioral strategy, preserving the five phases, although it affected the locations of transition points. In general, pushing wind delayed and pulling wind advanced phase transitions along the task progress axis (Fig. 7*A*; Table 2). The two sensory variables, Δt_{onset} and $\Delta\theta_{onset}$, continued carrying significant information on pole location under wind conditions, although not to the same extent (Fig. 7*B*). The amount of information carried by $\Delta\theta_{onset}$ decreased in both wind conditions, whereas that carried by Δt_{onset} slightly decreased in the pulling wind condition but increased in pushing wind. Increased information by Δt_{onset} was especially surprising in light of the general reduction in the overall range of Δt_{onset} values (no wind condition: 0.5 ± 84.5, pushing wind condition: 7.6 ± 54, $p = 1.3 \times 10^{-11}$; pulling wind condition: 18.8 ± 63; $p = 1.3 \times 10^{-4}$, Levene's test for variance equality; Fig. 7*C*). This increase in arrangement-wise separation, despite of an overall decrease in range, suggests a specific control strategy targeted at maximizing the sensitivity of Δt_{onset}. On the contrary, while the variability range of $\Delta\theta_{onset}$ was not significantly different between the no wind and pushing wind conditions (no wind condition: -8 ± 13; pushing wind condition: -15.3 ± 13, $p = 0.78$; pulling wind condition: -13.9 ± 10.2, $p = 7.9 \times 10^{-14}$, Levene's test for variance equality; Fig. 7*D*), the associated information decreased in pushing and more in pulling wind conditions, although it was still significant.

Controlled and modulated variables

To reveal the nature of motor-sensory adaptation that allowed our rats to overcome wind perturbation, we analyzed how wind affected the distributions of head and whisker motion variables and of the resulting contact variables. Variables were parsed such that each measured data point was assigned to a category based on the specific combination of arrangement (1, 2, 3, or no poles), correct/incorrect trial, whisker ID (C1 and C2, right or left), head position along the localization X range (x_H; from 1 to 7 cm with bins of 1 cm), and contact type (long/short). For example, one of the categories included all data point of a variable, in which arrangement was 1, rat's choices were correct, the analyzed whisker was right C2, the head was at 2 cm $< x_H <$ 3 cm and the contact was short. Different variables had different number of categories depending on their relation to the various components of the task (e.g., contact variables were assigned to 1 of 3 arrangement categories (arrangements 1, 2, 3), whereas whisker variables were also assigned to a fourth arrangement category of no poles trials). Categories of <20 data points were excluded (Table 3). Within the remaining categories, we ran an ANOVA test to establish the significance of wind effect. The resulting *p* values are presented in Figure 8*A*, where each curve corresponds to all category comparisons of an individual variable, in an ascending

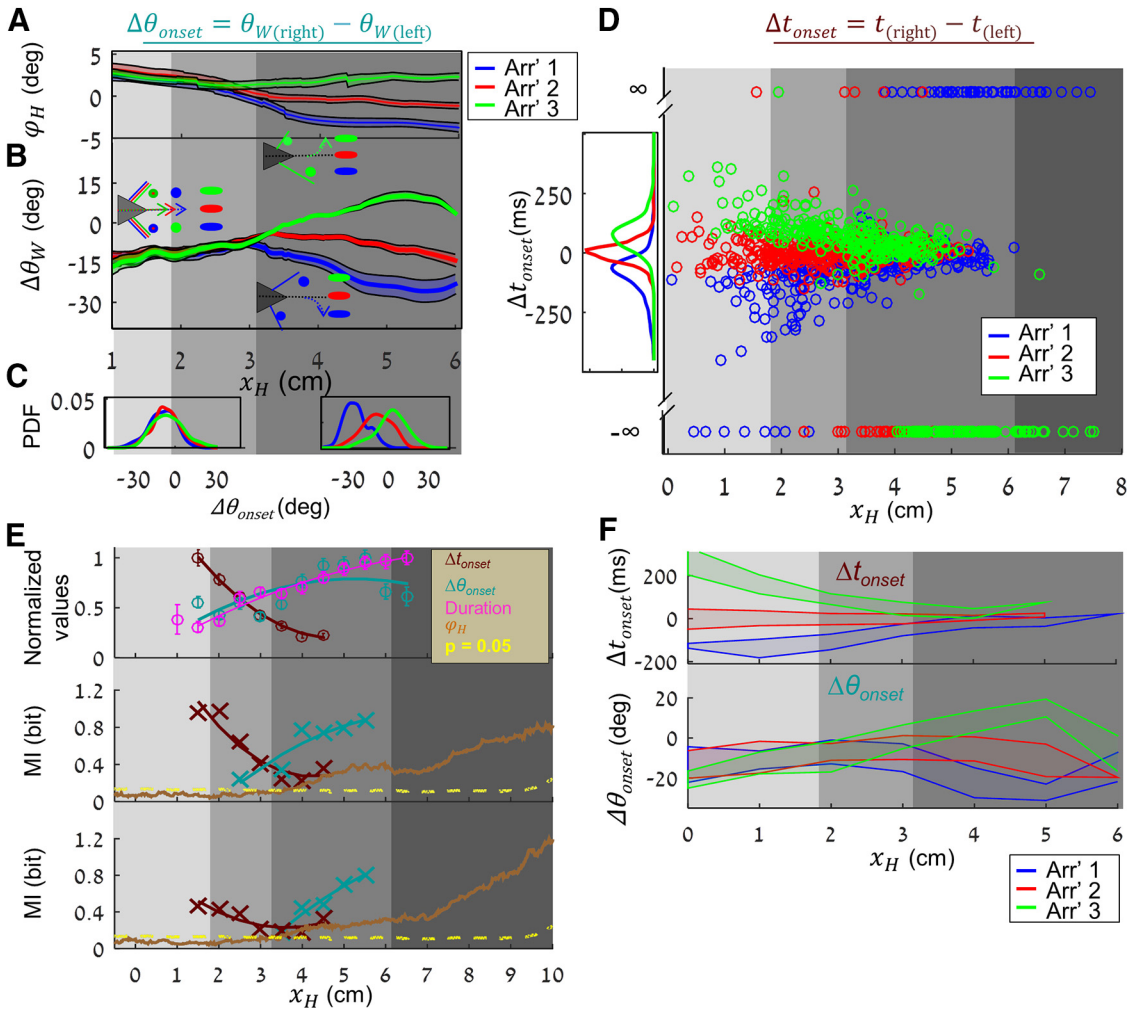

Figure 6. Temporal and spatial information cues. Head azimuth (φ_H) (***A***) and bilateral angle difference ($\Delta\theta_W$) (mean ± SEM) (***B***) along task progress in arrangements 1–3 (blue, red, green) trials. Gray shadings represent early (light) and late (dark) localization phases. Schemes illustrate whiskers' positions relative to the poles at different arrangements (same color code) at the relevant phase along task progress. ***C***, $\Delta\theta_{onset}$ distributions at early and late localization phases of 1–3 trial arrangements (blue, red, and green). ***D***, Δt_{onset} values along task progress, measured in arrangements 1–3 (blue, red, and green). Gray shadings represent detection, early and late localization, and choice execution phases. ***E***, Normalized values (mean ± SD) of Δt_{onset} (dark red), $\Delta\theta_{onset}$ (cyan), and contact duration (magenta) along 0.5 cm bins of task progress. Mutual information values (symbols) and trend lines by Δt_{onset} (dark red), $\Delta\theta_{onset}$ (cyan), and head azimuth (φ_H, brown) with trial arrangement (middle plot) and sipper selection (bottom plot), along task progress. Dashed yellow line indicates $p = 0.05$. ***F***, Patches are Δt_{onset} (top) and $\Delta\theta_{onset}$ (bottom) IQR in correct trials of arrangements 1–3 (blue, red, green).

Table 2. *x* coordinates (cm) of transition between consequent phases (CV13/CV12)

	Phases 1 and 2	Phases 2 and 3	Phases 3 and 4
No wind condition	1.7/1.9	3.0/3.5	6.4/6.0
Pushing wind condition	3.0/3.5	4.0/4.0	6.4/6.5
Pulling wind condition	1.6/1.7	3.0/3.0	6.0/6.2

order: for every variable (curve), categories of smallest *p* values (representing significant difference between conditions) were positioned on the left side of the *x*-axis. Thus, variables whose curves crossed the significance level line closer to the left side (indicating that, in most of their subgroups, there was no significant effect of condition) were considered to be more preserved, or more "controlled."

Table 3 lists the analyzed variables ordered by the value of their crossing point, where lower values indicate stronger invariance against external perturbations. We grouped the variables according to the modes in the distributions of their crossing points (the crossing points of the variables contained in Groups I-III are depicted in Fig. 8*A*, inset). Groups I and II contain variables that were maintained relatively invariant to wind perturbations and are here referred to as "controlled variables." These include 4 tightly controlled variables (Table 3, Group I): the duration of retraction and the duration of short contacts, radial distance of short contacts, and head azimuth during short contacts. Controlled variables with somewhat lower invariance include whisker protraction variables (amplitude, velocity, and duration), retraction amplitude and velocity, head azimuth during long contacts, and the radial distance of long contacts (Table 3, Group II).

Groups III, IV, and V contain variables that were significantly modulated in response to wind perturbations; we classify them as "modulated variables" (i.e., variables that were modulated to maintain the controlled variables in their desired ranges). They included head position along the *y*-axis and velocity along the *x*- and *y*-axes, whisker peak protraction and retraction angles, and duration of long contacts.

We next analyzed the major sources of variability and the dynamics of these measured variables; three representative examples are presented in Fig. 8*B–G*. Protraction whisker velocity, $\dot{\theta}_{W,max}$, was gradually reduced during the detection and maintained small and constant over the early and late localization

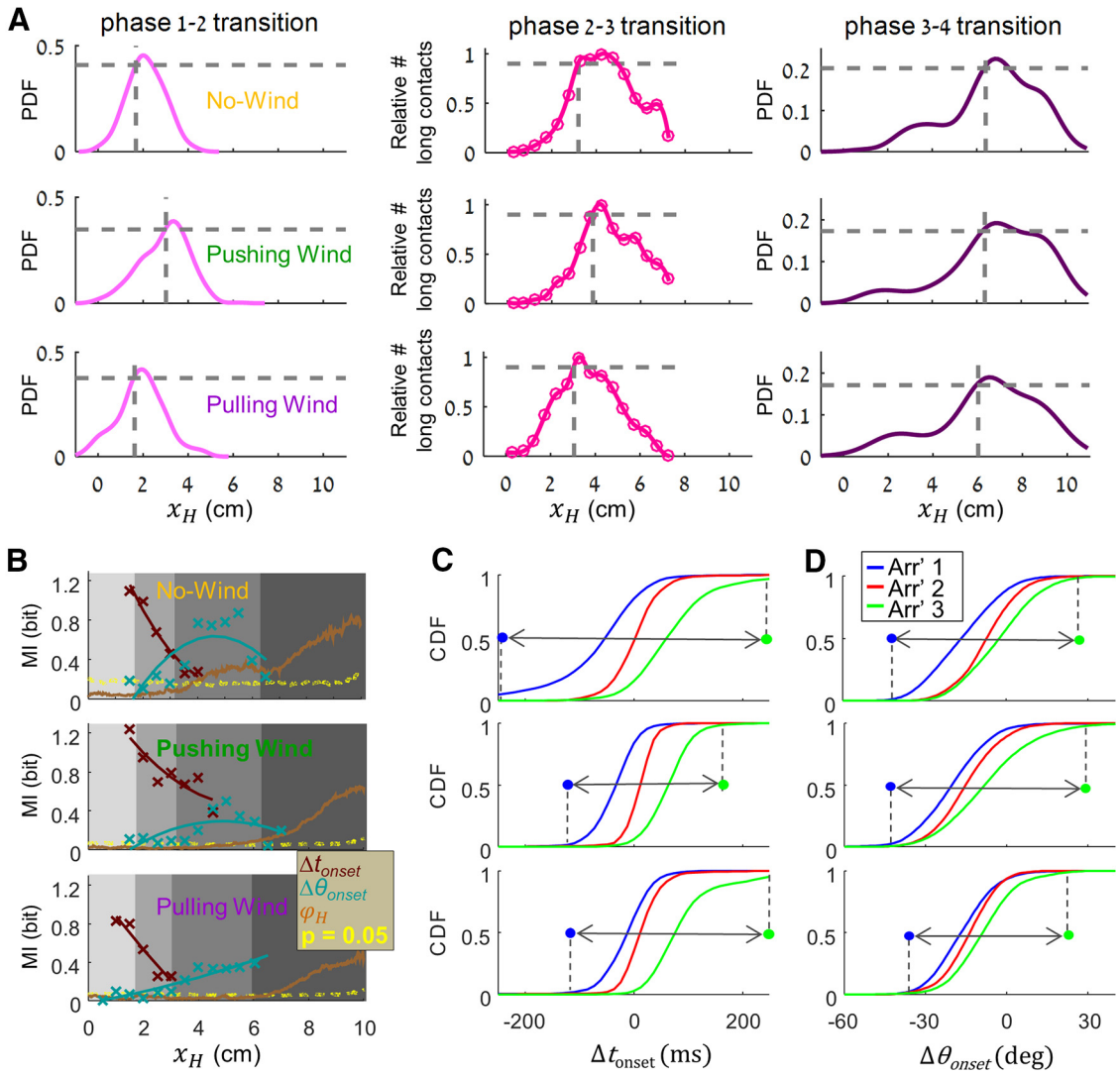

Figure 7. Wind effect. ***A***, Behavioral phase transition (columns) in the different wind conditions (rows; no wind; pushing wind; pulling wind) as defined for CV13 by the variables described in Figure 4*H* (see Materials and Methods). Vertical dashed gray lines indicate the locations of phase transitions along task progress. ***B***, Mutual information (symbols) and trend lines between Δt_{onset} (dark red), $\Delta\theta_{onset}$ (cyan), φ_H (brown), and trial arrangement along task progress, calculated for pulled data of (top to bottom) no wind, pushing wind, and pulling wind sessions. ***C***, Cumulative density distributions (CDF) of Δt_{onset} and in arrangements 1–3 (blue, red, and green, respectively), measured under (top to bottom) no wind, pushing wind, and pulling wind conditions. Colored symbols represent the 5th and 95th percentiles of values' ranges (pulled over all arrangements). Gray arrows represent the corresponding Δt_{onset} range. ***D***, Same as ***C*** for $\Delta\theta_{onset}$.

phases (Fig. 8*B*). We compared the variance contributed by condition, arrangement, and whisker ID, using *F* statistics. Large *F* values indicate a large contribution to the overall variance. In the case of whisker velocity ($\dot{\theta}_{W,max}$), most of the variability was contributed by whisker ID (Fig. 8*C*), but there was very little effect of arrangement and condition on the variability in the data. Head azimuth (φ_H) was maintained near 0 until late localization across all arrangements and conditions, especially during early localization (as demonstrated by the troughs in *F* statistics related to arrangement and condition; Fig. 8*D*,*E*; note the log scale of *y*-axis).

In contrast to the controlled variables, modulated variables exhibited significant changes across conditions. For example, rats elevated whisking peak angle ($\theta_{w,max}$) in pushing and more in pulling wind conditions (Fig. 8*F*) while maintaining a rather fixed and small variance range within each wind condition.

Our basic assumption was that motor variables are controlled in a way that optimizes perception. Two coding sensory variables were identified in these experiments: Δt_{onset} and $\Delta\theta_{onset}$ (Fig. 6). Both variables, and to a greater extent Δt_{onset}, exhibited resilience to wind perturbation (Fig. 7*B–D*). We thus examined the dependency of these coding variables on motor controlled variables. Both coding variables (and more so Δt_{onset}) depended significantly on the values of the two representative controlled variables: whisker velocity and head azimuth (Figs. 8*H*,*I*, two left columns). In contrast, these coding variables did not depend on modulated variables (e.g., on $\theta_{W,max}$; Figs. 8*H*,*I*, right column).

Discussion

That perception involves gradual accumulation of sensory data had been repeatedly shown (Romo and Salinas, 2001, 2003; Mazurek et al., 2003; Gold and Shadlen, 2007). This, however, was typically shown in tasks during which the sensory variables, as well as their acquisition time frame, were dictated by the experimental design. In contrast, in natural or natural-like conditions, subjects select sensory variables actively via specific motor strategies (Munz et al., 2010). This approach of imposing minimal

Table 3. All analyzed variables sorted by invariance[a]

Group	Variable	CP	No. of subgroups	Mean samples/ subgroup	Mean samples/ group
I	$T_{W,ret}$	0.10	371	135.94	109.36
	T_{C_S}	0.10	50	36.26	
	r_{C_S}	0.10	33	32.1	
	φ_{H,C_S}	0.10	50	36.26	
II	$T_{W,prt}$	0.60	376	134.51	131.47
	$A_{W,ret}$	0.80	371	135.94	
	$A_{W,prt}$	1.10	376	134.51	
	$\bar{\theta}_{W,ret}$	1.20	371	135.94	
	$\bar{\theta}_{W,prt}$	1.30	376	134.51	
	r_{C_L}	1.60	49	39.2	
	$\dot{\theta}_{W,max}$	1.70	376	134.51	
	$\dot{\theta}_{W,min}$	1.80	371	135.94	
	φ_{H,C_L}	2.70	59	46.29	
III	T_{C_L}	7.40	59	46.29	111.45
	$\dot{y}_H$	7.80	96	151.49	
IV	y_H	15.90	96	151.56	141.26
	$\theta_{W,min}$	19.60	371	135.94	
	$\dot{x}_H$	20.90	96	151.49	
V	$\theta_{W,max}$	27.10	376	134.51	134.51

[a]CP, "crossing point" (Fig. 8*A*): % of subgroups below $p = 0.0001$.

constrains exposed a common meta-design of task solving by our rats. They started by detecting the presence of the poles, continued with acquiring temporal sensory variables (Δt_{onset}) during the early localization phase, then spatial sensory variables ($\Delta\theta_{onset}$) during late localization phase, and then proceeded toward the appropriate sipper (Fig. 4). This strategy included a priori setting of motor variables in their relevant working ranges. For example, when reaching to the localization zone, even before any contact occurred, the rats reduced their whisking angle and velocity significantly (Figs. 4*G*, 8*B*,*F*), the latter likely to increase temporal resolution. Such predictive motor behavior could be imprinted in motor networks at early stages of task learning (Kuhlman et al., 2014) in a way that also presets sensory networks to the relevant working ranges (Pais-Vieira et al., 2013).

Indeed, during early localization, contacts were kept short and temporal information (mutual information by Δt_{onset}) was kept high, in agreement with temporal coding by bilateral first spike delays (Arabzadeh et al., 2006; Ahissar and Knutsen, 2008; Petersen et al., 2009). During the late localization phase, whisker-pole contacts were long and angular information ($\Delta\theta_{onset}$) gradually increased (Fig. 6). Long contact durations support the use of "morphological coding," such as the relationship between whisker curvature and angle (Bagdasarian et al., 2013; Quist et al., 2014) for perceiving object location because the reliability of morphological coding increases with contact duration (Bagdasarian et al., 2013). These morphological relationships are translated to mechanical stresses that are sensible by follicle mechanoreceptors in a way that determines object localization (Pammer et al., 2013). Such transition from one coding variable to another may be associated with multiple-code neuronal processing at the relevant (e.g., thalamocortical) levels (Yu et al., 2015). Naturally, however, part of the involved variables (e.g., forces at the follicle) could not be measured directly or estimated indirectly (e.g., by measuring whisker curvature) in this study due to technical limitations.

The short contacts described here are in agreement with an active control aimed at "minimal impingement" (Mitchinson et al., 2007). Such control may be an open-loop one, simply ensuring short-duration protractions; or closed-loop one, inducing retraction immediately upon contact (Deutsch et al., 2012). The long contacts described here are assumed to be controlled differently. Our rats had to pass the poles to reach the reward and could not avoid contacting the poles while moving forward, which resulted in relatively long contacts with strong impingements.

We focused our analysis on the relative variables Δt_{onset} and $\Delta\theta_{onset}$. In principle, rats could also solve the task by independently localizing the objects in both sides ("absolute" localization; Mehta et al., 2007; O'Connor et al., 2010) and computing the difference centrally. We find this possibility less likely given the lower resolution of "absolute" localization (Diamond et al., 2008) and the significant amount of information conveyed by the relative variables here (Figs. 6, 7).

Adaptation to wind perturbation and controlled variables

In natural conditions, perception typically involves active acquisition of sensory data. Such acquisition requires a coordination of motor variables and sensory coding variables, in a manner that facilitates the acquisition of perceptually relevant information (Ko et al., 2010; Boubenec et al., 2012; Kuang et al., 2012; Quist and Hartmann, 2012; Bagdasarian et al., 2013; Hires et al., 2013; Pammer et al., 2013). Because motor variables are readily modulated in perceptual time scales, whereas sensory coding is modifiable on much slower time scales (Saig et al., 2012), motor control is apt to enable perceptual resilience to environmental changes.

Our rats managed to keep their perceptual precision when facing pushing wind (Fig. 3). Our analysis revealed that in this condition the amount of information carried by the temporal sensory variable (Δt_{onset}) actually increased, compared with no wind, despite a significant decrease of its values range (Fig. 7*B*,*C*). This was in contrast to the decrease in the amount of information carried by the spatial sensory variable ($\Delta\theta_{onset}$) in this condition. The improvement in the reliability of Δt_{onset} likely resulted from an active adaptation of the rat's perceptual strategy in response to the change in environmental conditions. Interestingly, our rats did not find a corresponding adapted strategy for the pulling wind condition (Fig. 7*B*), which eventually resulted in impaired performance (Fig. 3*A*). Importantly, the fact that rats significantly increased peak whisking angles and set-points in both wind directions (Fig. 8*F*) excluded the possibility that all observed behavioral differences merely reflect mechanical effects of the wind.

While adapting to wind perturbations, our rats selectively maintained the motor variables affecting the temporal and spatial codes (controlled variables) in their working ranges during the relevant behavioral phases. The primary variables affecting temporal coding were head azimuth and whiskers velocity during protraction. Aligned head azimuth (0 degrees) ensured balanced bilateral comparison, and whisker velocity determined sensory resolution (Gamzu and Ahissar, 2001; Saig et al., 2012; Weber et al., 2013). Accordingly, these variables were kept invariant during early localization (Fig. 8*B–E*), which indeed maintained the coding power of Δt_{onset} (Fig. 7*B*). The other controlled variables observed here are related to either whisking amplitude ($A_{W,ret}$;$A_{W,prt}$), whisking duration ($T_{W,ret}$;$T_{W,prt}$), or whiskers-poles contacts (r_{C_S};r_{C_L}). Control of whisking amplitude and duration may be either a byproduct of controlling whisking velocity (Deutsch et al., 2012) or serving other purposes not specific to the task at hand. Contact-related variables may affect whiskers morphological based location coding (Bagdasarian et al., 2013).

Head azimuth was controlled also during late localization (φ_H,c_L), as a means to keep coding by $\Delta\theta_{onset}$ informative. Interestingly, the control of head azimuth was tighter during wind

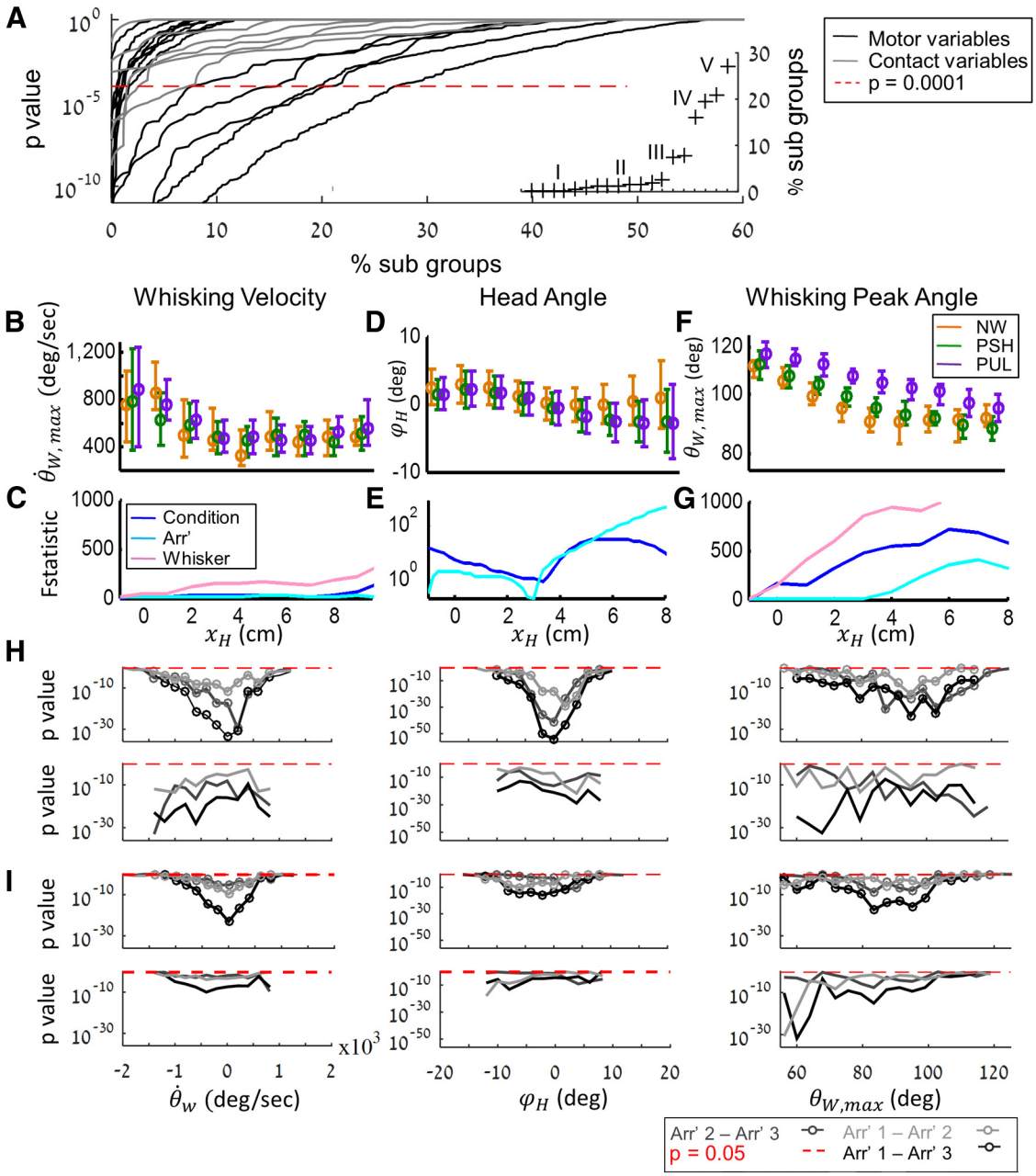

Figure 8. Invariance and modulation of variables. ***A***, *p* values calculated to establish difference due to condition among subgroups of motor (black) and contact (gray) variables. Inset, Point of crossing the $p = 0.0001$ level for individual variables. Labels indicate the groups assigned in Table 3. ***B***, Whisking velocity ($\dot{\theta}_{W,max}$; median ± IQR) along task progress under no wind (NW, orange), pushing wind (PSH, green), and pulling wind (PUL, purple) conditions. ***C***, Calculated variance in $\dot{\theta}_{W,max}$ data (*F* statistics) due to condition (blue), arrangement (cyan), and whisker ID (pink) along task progress. ***D***, ***E***, Same as ***B***, ***C*** for head azimuth (φ_H) and ***F***, ***G*** peak whisker angle ($\theta_{W,max}$). ***H***, *p* values of the pairwise comparison (ANOVA) between Δt_{onset} values, measured in arrangements 1 and 2 (light gray), 2 and 3 (dark gray), or 1 and 3 (black) over the bins of the abscissa variable (left to right: whisker velocity $\dot{\theta}_{W,max}$, head azimuth φ_H, and peak whisker angle $\theta_{W,max}$). Red dashed line indicates 0.05 significance line. Over these bins, the curves assess the strength of Δt_{onset} in separating arrangements (lower *p* values indicate better separation). Top, Separation quality (*p* value). Bottom, Shuffling control: an equal number of values from each arrangement were randomly selected in each bin to compose a dataset of 102 samples. Their assignments to values of the abscissa were shuffled, but not their assignments to arrangement. *p* values were recalculated, and the procedure was repeated 100 times. The curves represent the lowest 5% *p* values in each bin across all repetitions. ***I***, Same as ***H*** but for $\Delta\theta_{onset}$.

conditions (data not shown), which may suggest that the extent of control the system implements is not constant but may change with respect to conditions: namely, that a stricter control scheme is applied when the task becomes more difficult or under more intense perturbation.

Motor-sensory-motor loops and perceptual constancy

The links shown here between sensory accuracy and reliability and the control of motor variables strongly suggest that motor and sensory variables are controlled together, as part of the same control loop. Several studies indicated that rodents operate their whiskers in a closed-loop manner, by which whisker motion depends on the incoming sensory data (Mitchinson et al., 2007; Deutsch et al., 2012; Bagdasarian et al., 2013). In the case of the vibrissal system, such loops are implemented via tight motor-object-sensory transformations (Bagdasarian et al., 2013) and several levels of sensory-motor pathways (Kleinfeld et al., 1999; Kleinfeld et al., 2006; Ahissar and Knutsen, 2008; Diamond et al.,

2008), which together compose a set of vibrissal motor-sensory-motor loops. We suggest that the control over controlled and modulated variables is done via these motor-sensory-motor loops and that these variables are relevant for perception (Simony et al., 2008).

Our results further suggest that this mechanism enables perceptual constancy: the resilience of perception to changes in the conditions affecting the interactions between the subject and the object. Perceptual constancy has been investigated in detail over more than a century (Gilchrist et al., 1999). It is generally accepted that the nervous system somehow "takes into account" the conditions affecting subject–object interactions (such as distance from an object for size perception and humidity for roughness perception), using some sort of sensory processing that corrects the presumably distorted proximal stimulus (Helmholtz, 1925; Hochberg, 1978; Wade and Swanston, 1996). Yet, dynamic and motor-sensory based schemes of perception (Port and Van Gelder, 1995; Kelso, 1997; Ahissar and Arieli, 2001; Freeman, 2001; O'Regan and Noe, 2001) offer an alternative mechanism, in which environmental conditions can be taken into account by an appropriate control over the motor variables that are relevant to acquire the sensory cues. In line with the latter, constancy of roughness perception was shown to occur with active sensing but not with passive sensing (Yoshioka et al., 2011), suggesting that motor variables play a significant role in maintaining tactile perceptual constancy.

We show here that while perceiving object location in different wind conditions rats maintain perceptual constancy (preserving reliable sensory coding) by the preservation of a set of coding-relevant "controlled variables" within certain ranges while modulating other, "modulated variables." This strategy minimized the distortion of perceptually relevant sensory variables (the "proximal stimulus") caused by environmental conditions, thereby enabling spatial perceptual constancy.

References

Ahissar E, Arieli A (2001) Figuring space by time. Neuron 32:185–201. CrossRef Medline

Ahissar E, Knutsen PM (2008) Object localization with whiskers. Biol Cybern 98:449–458. CrossRef Medline

Anjum F, Turni H, Mulder PG, van der Burg J, Brecht M (2006) Tactile guidance of prey capture in Etruscan shrews. Proc Natl Acad Sci U S A 103:16544–16549. CrossRef Medline

Arabzadeh E, Panzeri S, Diamond ME (2006) Deciphering the spike train of a sensory neuron: counts and temporal patterns in the rat whisker pathway. J Neurosci 26:9216–9226. CrossRef Medline

Bagdasarian K, Szwed M, Knutsen PM, Deutsch D, Derdikman D, Pietr M, Simony E, Ahissar E (2013) Pre-neuronal morphological processing of object location by individual whiskers. Nat Neurosci 16:622–631. CrossRef Medline

Boubenec Y, Shulz DE, Debrégeas G (2012) Whisker encoding of mechanical events during active tactile exploration. Front Behav Neurosci 6:74. CrossRef Medline

Brecht M, Preilowski B, Merzenich MM (1997) Functional architecture of the mystacial vibrissae. Behav Brain Res 84:81–97. CrossRef Medline

Carvell GE, Simons DJ (1990) Biometric analyses of vibrissal tactile discrimination in the rat. J Neurosci 10:2638–2648. Medline

Deutsch D, Pietr M, Knutsen PM, Ahissar E, Schneidman E (2012) Fast feedback in active sensing: touch-induced changes to whisker-object interaction. PLoS One 7:e44272. CrossRef Medline

Diamond ME (2010) Texture sensation through the fingertips and the whiskers. Curr Opin Neurobiol 20:319–327. CrossRef Medline

Diamond ME, von Heimendahl M, Knutsen PM, Kleinfeld D, Ahissar E (2008) 'Where' and 'what' in the whisker sensorimotor system. Nat Rev Neurosci 9:601–612. CrossRef Medline

Freeman W (2001) How brains make up their minds. New York: Columbia UP.

Gamzu E, Ahissar E (2001) Importance of temporal cues for tactile spatial-frequency discrimination. J Neurosci 21:7416–7427. Medline

Gilchrist A, Kossyfidis C, Bonato F, Agostini T, Cataliotti J, Li X, Spehar B, Annan V, Economou E (1999) An anchoring theory of lightness perception. Psychol Rev 106:795–834. CrossRef Medline

Gold JI, Shadlen MN (2007) The neural basis of decision making. Annu Rev Neurosci 30:535–574. CrossRef Medline

Grant RA, Mitchinson B, Prescott TJ (2012) The development of whisker control in rats in relation to locomotion. Dev Psychobiol 54:151–168. CrossRef Medline

Helmholtz H (1925) Helmholtz's treatise on physiological optics, Vol 3. Trans JPC Southall. New York: Optical Society of America.

Hires SA, Pammer L, Svoboda K, Golomb D (2013) Tapered whiskers are required for active tactile sensation. eLife 2:e01350. CrossRef Medline

Hochberg J (1978) Perceptual constancy. Science 201:1218–1219. CrossRef Medline

Kelso JS (1997) Dynamic patterns: the self-organization of brain and behavior. Cambridge, MA: Massachusetts Institute of Technology.

Kleinfeld D, Berg RW, O'Connor SM (1999) Anatomical loops and their electrical dynamics in relation to whisking by rat. Somatosens Mot Res 16:69–88. CrossRef Medline

Kleinfeld D, Ahissar E, Diamond ME (2006) Active sensation: insights from the rodent vibrissa sensorimotor system. Curr Opin Neurobiol 16:435–444. CrossRef Medline

Knutsen PM, Ahissar E (2009) Orthogonal coding of object location. Trends Neurosci 32:101–109. CrossRef Medline

Knutsen PM, Derdikman D, Ahissar E (2005) Tracking whisker and head movements in unrestrained behaving rodents. J Neurophysiol 93:2294–2301. CrossRef Medline

Knutsen PM, Pietr M, Ahissar E (2006) Haptic object localization in the vibrissal system: behavior and performance. J Neurosci 26:8451–8464. CrossRef Medline

Ko HK, Poletti M, Rucci M (2010) Microsaccades precisely relocate gaze in a high visual acuity task. Nat Neurosci 13:1549–1553. CrossRef Medline

Kuang X, Poletti M, Victor JD, Rucci M (2012) Temporal encoding of spatial information during active visual fixation. Curr Biol 22:510–514. CrossRef Medline

Kuhlman SJ, O'Connor DH, Fox K, Svoboda K (2014) Structural plasticity within the barrel cortex during initial phases of whisker-dependent learning. J Neurosci 34:6078–6083. CrossRef Medline

Maravall M, Diamond ME (2014) Algorithms of whisker-mediated touch perception. Curr Opin Neurobiol 25:176–186. CrossRef Medline

Mazurek ME, Roitman JD, Ditterich J, Shadlen MN (2003) A role for neural integrators in perceptual decision making. Cereb Cortex 13:1257–1269. CrossRef Medline

Mehta SB, Whitmer D, Figueroa R, Williams BA, Kleinfeld D (2007) Active spatial perception in the vibrissa scanning sensorimotor system. PLoS Biol 5:e15. CrossRef Medline

Mitchinson B, Martin CJ, Grant RA, Prescott TJ (2007) Feedback control in active sensing: rat exploratory whisking is modulated by environmental contact. Proc Biol Sci 274:1035–1041. CrossRef Medline

Munz M, Brecht M, Wolfe J (2010) Active touch during shrew prey capture. Front Behav Neurosci 4:191. CrossRef Medline

O'Connor DH, Clack NG, Huber D, Komiyama T, Myers EW, Svoboda K (2010) Vibrissa-based object localization in head-fixed mice. J Neurosci 30:1947–1967. CrossRef Medline

O'Regan JK, Noe A (2001) A sensorimotor account of vision and visual consciousness. Behav Brain Sci 24:939–973; discussion 973–1031.

Pais-Vieira M, Lebedev MA, Wiest MC, Nicolelis MA (2013) Simultaneous top-down modulation of the primary somatosensory cortex and thalamic nuclei during active tactile discrimination. J Neurosci 33:4076–4093. CrossRef Medline

Pammer L, O'Connor DH, Hires SA, Clack NG, Huber D, Myers EW, Svoboda K (2013) The mechanical variables underlying object localization along the axis of the whisker. J Neurosci 33:6726–6741. CrossRef Medline

Petersen RS, Panzeri S, Maravall M (2009) Neural coding and contextual influences in the whisker system. Biol Cybern 100:427–446. CrossRef Medline

Port RF, Van Gelder T (1995) Mind as motion: explorations in the dynamics of cognition. Cambridge, MA: Massachusetts Institute of Technology.

Prescott TJ, Diamond ME, Wing AM (2011) Active touch sensing. Philos Trans R Soc Lond B Biol Sci 366:2989–2995. CrossRef Medline

Quist BW, Hartmann MJ (2012) Mechanical signals at the base of a rat vibrissa: the effect of intrinsic vibrissa curvature and implications for tactile exploration. J Neurophysiol 107:2298–2312. CrossRef Medline

Quist BW, Seghete V, Huet LA, Murphey TD, Hartmann MJ (2014) Modeling forces and moments at the base of a rat vibrissa during noncontact whisking and whisking against an object. J Neurosci 34:9828–9844. CrossRef Medline

Ritt JT, Andermann ML, Moore CI (2008) Embodied information processing: vibrissa mechanics and texture features shape micromotions in actively sensing rats. Neuron 57:599–613. CrossRef Medline

Romo R, Salinas E (2001) Touch and go: decision-making mechanisms in somatosensation. Annu Rev Neurosci 24:107–137. CrossRef Medline

Romo R, Salinas E (2003) Flutter discrimination: neural codes, perception, memory and decision making. Nat Rev Neurosci 4:203–218. CrossRef Medline

Saig A, Gordon G, Assa E, Arieli A, Ahissar E (2012) Motor-sensory confluence in tactile perception. J Neurosci 32:14022–14032. CrossRef Medline

Shadmehr R, Smith MA, Krakauer JW (2010) Error correction, sensory prediction, and adaptation in motor control. Annu Rev Neurosci 33:89–108. CrossRef Medline

Simony E, Saraf-Sinik I, Golomb D, Ahissar E (2008) Sensation-targeted motor control: every spike counts? Focus on: "Whisker movements evoked by stimulation of single motor neurons in the facial nucleus of the rat." J Neurophysiol 99:2757–2759. CrossRef

Todorov E (2004) Optimality principles in sensorimotor control. Nat Neurosci 7:907–915. CrossRef Medline

Towal RB, Hartmann MJ (2008) Variability in velocity profiles during free-air whisking behavior of unrestrained rats. J Neurophysiol 100:740–752. CrossRef Medline

Voigts J, Herman DH, Celikel T (2015) Tactile object localization by anticipatory whisker motion. J Neurophysiol 113:620–632. CrossRef Medline

von Heimendahl M, Itskov PM, Arabzadeh E, Diamond ME (2007) Neuronal activity in rat barrel cortex underlying texture discrimination. PLoS Biol 5:e305. CrossRef Medline

Wade NJ, Swanston MT (1996) A general model for the perception of space and motion. Perception 25:187–194. CrossRef Medline

Weber AI, Saal HP, Lieber JD, Cheng JW, Manfredi LR, Dammann JF 3rd, Bensmaia SJ (2013) Spatial and temporal codes mediate the tactile perception of natural textures. Proc Natl Acad Sci U S A 110:17107–17112. CrossRef Medline

Wolfe J, Hill DN, Pahlavan S, Drew PJ, Kleinfeld D, Feldman DE (2008) Texture coding in the rat whisker system: slip-stick versus differential resonance. PLoS Biol 6:e215. CrossRef Medline

Yoshioka T, Craig JC, Beck GC, Hsiao SS (2011) Perceptual constancy of texture roughness in the tactile system. J Neurosci 31:17603–17611. CrossRef Medline

Yu C, Horev G, Rubin N, Derdikman D, Haidarliu S, Ahissar E (2015) Coding of object location in the vibrissal thalamocortical system. Cereb Cortex 25:563–577. CrossRef Medline